



Title	Two-component optical conductivity in the cuprates: A necessary consequence of preformed pairs
Author(s)	Dan, WL; Guo, H; Chien, CC; Levin, K
Citation	Physical Review B, 2012, v. 86, p. 134518:1-6
Issued Date	2012
URL	http://hdl.handle.net/10722/181698
Rights	Physical Review B. Copyright © American Physical Society.

Two-component optical conductivity in the cuprates: A necessary consequence of preformed pairsDan Wulin,¹ Hao Guo,² Chih-Chun Chien,³ and K. Levin¹¹*James Franck Institute and Department of Physics, University of Chicago, Chicago, Illinois 60637, USA*²*Department of Physics, University of Hong Kong, Hong Kong, China*³*Theoretical Division, Los Alamos National Laboratory, MS B213, Los Alamos, New Mexico 87545, USA*

(Received 23 August 2011; revised manuscript received 9 September 2012; published 17 October 2012)

We address how the finite frequency real conductivity $\sigma(\omega)$ in the underdoped cuprates is affected by the pseudogap, contrasting the behavior above and below T_c . The f-sum rule is analytically shown to hold. Here we presume the pseudogap is associated with noncondensed pairs arising from stronger-than-BCS attraction. This leads to both a Drude and a midinfrared peak, the latter associated with the energy needed to break pairs. These general characteristics appear consistent with experiment. Importantly, there is no more theoretical flexibility (phenomenology) here than in BCS theory; the origin of the two component conductivity we find is robust.

DOI: [10.1103/PhysRevB.86.134518](https://doi.org/10.1103/PhysRevB.86.134518)

PACS number(s): 74.20.-z, 74.72.-h

I. INTRODUCTION

The behavior of the in-plane ac conductivity $\sigma(\omega)$ in the underdoped high-temperature superconductors has raised a number of puzzles¹ for theoretical scenarios surrounding the origin of the mysterious pseudogap. At the same time, there has been substantial recent progress in establishing experimental constraints on the interplay of the pseudogap and $\sigma(\omega)$.² A key feature of $\sigma(\omega)$ is its two component nature consisting of a “coherent” Drude-like low- ω feature followed by an approximately T -independent midinfrared (MIR) peak.¹⁻³ The latter “extends to the pseudogap boundary in the phase diagram at T^* . Moreover a softening of the MIR band with doping [scales with] the decrease in the pseudogap temperature T^* .”² Crucial to this picture is that “high T_c materials are in the clean limit and that ... the MIR feature is seen above and below T_c .”⁴ Thus, it appears that this feature is not associated with disordered superconductivity and related momentum nonconserving processes, but rather it is “due to the unconventional nature of the [optical] response.”¹

It is the purpose of this paper to address these related observations in the context of a preformed pair Gor'kov-based theory that extends BCS theory to the strong attraction limit.⁵ The theoretical basis was presented in more detail in the previous accompanying paper and even earlier in the literature^{6,7} at a more microscopic level. Our expressions for $\sigma(\omega)$ are equivalent to their BCS analog when the pseudogap vanishes.

At its core, this approach is microscopically based, and the level of phenomenological flexibility^{8,9} is no more than that associated with transport in strict BCS superconductors. Alternative mechanisms for the two-component optical response include Mott-related physics¹⁰ and d-density wave¹¹ approaches, which have acknowledged inconsistencies,¹² as well as approaches that build on inhomogeneity effects.¹³ Distinguishing our approach is its very direct association with the pseudogap. In an evidently less transparent way, a two-component response arises numerically¹⁰ in the presence of Mott-Hubbard correlations above T_c . However, experiments show how the MIR feature must persist in the presence of superconductivity, suggesting that pseudogap physics affects superconductivity below T_c , as found here.

Unique is our capability to address both the normal (pseudogap) and superconducting phases. Moreover, we are also able to establish^{8,9} compatibility with the transverse f-sum rule without problematic negative conductivity¹⁰ contributions. Finally, our approach is to be distinguished from the phase fluctuation scenario that appears problematic in light of recent optical data related to the imaginary THz conductivity.¹⁴ In experimental support of our scenario is the claim based on $\sigma(\omega)$ data¹⁵ that the “doping dependence suggests a smooth transition from a BCS mode of condensation in the overdoped regime to a different mode in underdoped samples, [as] in the case of a BCS to Bose-Einstein crossover.”

Our analysis leads to the following physical picture: The presence of noncondensed pairs both above and below T_c yields an MIR peak. This peak occurs around the energy needed to break pairs and thereby create conducting fermions. Its position is doping dependent, and only weakly temperature dependent, following the weak T dependence of the excitation gap $\Delta(T)$. The relatively high-frequency spectral weight from these pseudogap effects, present in the normal phase, is transferred to the condensate as T decreases below T_c , leading to a narrowing of the low ω Drude feature, as appears to be experimentally observed. Even relatively poor samples are in the clean limit,^{1,4} so that an alternative pair creation/annihilation contribution associated with broken translational invariance cannot be invoked to explain the observed MIR absorption.

Before doing detailed calculations, it is possible to anticipate the behavior of $\sigma(\omega)$ at a physical level. In addition to the $\omega \equiv 0$ condensate contribution, the $\omega \neq 0$ conductivity consists of two terms, the more standard one associated with scattering of fermionic quasiparticles and the other associated with the breaking of the pairs. The term associated with the scattering of fermionic quasiparticles gives rise to the usual Drude peak. In the presence of stronger than BCS attraction, we observe this second contribution, a novel pair breaking effect of the pseudogap. It reflects processes that require a minimal frequency of the order of $2\Delta(T)$. We associate this term with the MIR peak. Sum rule arguments imply that the larger this MIR peak is, the smaller the $\omega \approx 0$ contribution becomes; that is, pseudogap effects lower the dc conductivity σ^{dc} .⁹ This transfer of spectral weight can be understood as deriving from the fact that when noncondensed pairs are

present, the number of fermions available for scattering is decreased; these fermions are tied up into pairs.

II. BACKGROUND THEORY

We note that the details of the background theory are presented in the companion paper. This work is based on earlier transport studies^{5,6,8} which address the current-current correlation function $\overleftrightarrow{\chi}_{JJ} = \overleftrightarrow{P} + \frac{\overleftrightarrow{n}}{m} - C_\chi$, where C_χ is associated with collective modes. The latter do not enter above T_c nor in the transverse gauge below T_c . Here \overleftrightarrow{P} is the paramagnetic and $\frac{\overleftrightarrow{n}}{m}$ the diamagnetic component. The real part of the conductivity can be extracted from $\overleftrightarrow{P}(Q)$ using the definition $\text{Re}\sigma(\omega \neq 0) \equiv -\lim_{q \rightarrow 0} \text{Im} P^{xx}(i\Omega_m \rightarrow \omega + i0^+, \mathbf{q})/\omega$.

For notational convenience we define $E \equiv E_{\mathbf{k}} \equiv \sqrt{\xi_{\mathbf{k}}^2 + \Delta^2}$ as the fermionic excitation spectrum, $\xi_{\mathbf{k}}$ is the normal state dispersion, $f \equiv f(E)$ is the Fermi distribution function, and the pairing gap $\Delta^2 = \Delta_{sc}^2 + \Delta_{pg}^2$ is found^{5,6} to contain both condensed (*sc*) and noncondensed (*pg*) terms. In the d-wave case, we write $\Delta_{\mathbf{k}} = \Delta\varphi_{\mathbf{k}}$, $\xi_{\mathbf{k}} = -2t(\cos k_x + \cos k_y) - \mu$, and $E_{\mathbf{k}} = \sqrt{\xi_{\mathbf{k}}^2 + \Delta_{\mathbf{k}}^2}$, where $\varphi_{\mathbf{k}} = (\cos k_x - \cos k_y)/2$ is the d-wave form factor.

The full expression for the current-current response kernel was discussed elsewhere^{8,9} and summarized in the accompanying paper. It has been derived microscopically from Maki-Thompson and Aslamazov Larkin diagrams⁶ as well as more directly as shown in the previous paper from Ward identities based on the pseudogap self-energy. We find

$$\overleftrightarrow{P}(Q) \approx 2 \sum_K \frac{\partial \xi_{\mathbf{k}+Q/2}}{\partial \mathbf{k}} \frac{\partial \xi_{\mathbf{k}+Q/2}}{\partial \mathbf{k}} [G_K G_{K+Q} + F_{sc,K} F_{sc,K+Q} - F_{pg,K} F_{pg,K+Q}]. \quad (1)$$

Here $Q = (\mathbf{q}, i\Omega_m)$, $i\Omega_m$ is a bosonic Matsubara frequency, and the three forms of propagators, introduced in earlier work⁹ are

$$G(K) = \left(i\omega_n - \xi_{\mathbf{k}} + i\gamma - \frac{\Delta_{pg,\mathbf{k}}^2}{i\omega_n + \xi_{\mathbf{k}} + i\gamma} - \frac{\Delta_{sc,\mathbf{k}}^2}{i\omega_n + \xi_{\mathbf{k}}} \right)^{-1},$$

$$F_{sc}(K) \equiv -\frac{\Delta_{sc,\mathbf{k}}}{i\omega_n + \xi_{\mathbf{k}}} \frac{1}{i\omega_n - \xi_{\mathbf{k}} - \frac{\Delta_{\mathbf{k}}^2}{i\omega_n + \xi_{\mathbf{k}}}},$$

$$F_{pg}(K) \equiv -\frac{\Delta_{pg,\mathbf{k}}}{i\omega_n + \xi_{\mathbf{k}} + i\gamma} G(K). \quad (2)$$

Here $K = (\mathbf{k}, i\omega_n)$ and $i\omega_n$ is the fermionic Matsubara frequency. Here γ represents the fermionic damping. This parameter was identified in the pseudogap self-energy very early on^{16,17} on the basis of a microscopic t-matrix theory where there is coupling only between particles and pairs. (All higher order couplings are ignored in generic t-matrix schemes). In this sense the parameter γ arises from the interconversion of fermions and noncondensed pairs. Importantly the noncondensed pairs are not abruptly affected by the onset of superconducting coherence. Rather, they are converted to condensed pairs as temperature is lowered. Because we include in effect two types of self-energies associated with the pseudogap and the condensate and because the condensate pairs are infinitely long lived, there is no natural physical

reason to contemplate changes in γ as T passes below T_c . Indeed, crucial to our physical picture is that our results appear robust with respect to γ without any detailed assumptions. General orders of magnitude for γ/Δ which we considered range from about 0.1 to 1.0, depending on the assumed doping level.

The first equation representing the full Green's function is associated with a BCS self-energy ($\propto \Delta_{sc}^2$) and a similar contribution from the noncondensed pairs ($\propto \Delta_{pg}^2$). The latter is fairly standard in the literature¹⁸⁻²⁰ and importantly was derived microscopically in our earlier work.¹⁶ This decomposition into condensed and noncondensed pair components was discussed in detail in the accompanying paper. Above, F_{sc} represents the usual Gorkov-like function associated with condensed pairs, and we can interpret F_{pg} as their noncondensed counterpart. The full excitation gap $\Delta(T)$ does not have a strong temperature dependence in the underdoped regime; below T_c this is because of a conversion of noncondensed to condensed pairs as T is reduced.

We may rewrite $\overleftrightarrow{P}(Q)$ in the regime of very weak dissipation ($\gamma \approx 0$) where the behavior is more physically transparent. For simplicity we will illustrate this result for s-wave pairing

$$\overleftrightarrow{P}(\omega, \mathbf{q}) = \sum_{\mathbf{k}} \frac{\mathbf{k}\mathbf{k}}{m^2} \left[\frac{E_+ + E_-}{E_+ E_-} (1 - f_+ - f_-) \times \frac{E_+ E_- - \xi_+ \xi_- - \delta\Delta^2}{\omega^2 - (E_+ + E_-)^2} - \frac{E_+ - E_-}{E_+ E_-} \times \frac{E_+ E_- + \xi_+ \xi_- + \delta\Delta^2}{\omega^2 - (E_+ - E_-)^2} (f_+ - f_-) \right], \quad (3)$$

where $f_{\pm} = f(E_{\pm})$ and $\delta\Delta^2 = \Delta_{sc}^2 - \Delta_{pg}^2$, $\xi_{\pm} = \xi_{\mathbf{k} \pm \mathbf{q}/2}$, and $E_{\pm} = E_{\mathbf{k} \pm \mathbf{q}/2}$. Importantly, one can analytically show that⁹ the transverse sum rule is precisely satisfied, as was summarized in the companion paper. This sum rule is intimately connected to the absence above T_c (and presence below) of a Meissner effect. The proof depends on the superfluid density, which at general temperatures is given by $n_s = (2/3)(\Delta_{sc}^2/m) \sum_{\mathbf{k}} k^2/E^2 [(1-2f)/2E + \partial f/\partial E]$. In addition, the total number of particles can be written as $n = \sum_{\mathbf{k}} [1 - \xi(1-2f)/E]$. In this way, it is seen⁹ that $\text{Re}\sigma(\omega \rightarrow 0) = (\pi n_s/m)\delta(\omega)$. Since $\Delta_{sc}^2 = \Delta^2 - \Delta_{pg}^2$, one can see that pseudogap effects, through Δ_{pg}^2 , act to lower the superfluid density; the excitation of these noncondensed pairs provides an additional mechanism, beyond the fermions, for depleting the condensate with increasing temperature. The different signs associated with the *pg* and *sc* contributions to the current response formally relate to vertex corrections of a different nature in the condensed and noncondensed components. Despite the simplicity of this expression, in no sense are vertex corrections to the bare polarization bubble ignored.

We introduce a transport lifetime $\tau = \gamma^{-1}$ into Eq. (3) via the replacement $\delta[\omega - (E_{\mathbf{k}}^+ \pm E_{\mathbf{k}}^-)] = \lim_{\tau \rightarrow \infty} \frac{1}{\pi} \frac{\frac{1}{\tau}}{[\omega - (E_{\mathbf{k}}^+ \pm E_{\mathbf{k}}^-)]^2 + \frac{1}{\tau^2}}$, to yield (for the more general

d-wave case)

$$\begin{aligned} \text{Re}\sigma(\omega \neq 0) = & \sum_{\mathbf{k}} 4\sin^2 k_x t^2 \left\{ \frac{\Delta_{\text{pg}}^2(T)\varphi_{\mathbf{k}}^2}{E_{\mathbf{k}}^2} \frac{1-2f(E_{\mathbf{k}})}{2E_{\mathbf{k}}} \right. \\ & \times \left[\frac{\tau}{1+(\omega-2E_{\mathbf{k}})^2\tau^2} + \frac{\tau}{1+(\omega+2E_{\mathbf{k}})^2\tau^2} \right] \\ & \left. - 2 \frac{E_{\mathbf{k}}^2 - \Delta_{\text{pg}}^2\varphi_{\mathbf{k}}^2}{E_{\mathbf{k}}^2} \frac{\partial f(E_{\mathbf{k}})}{\partial E_{\mathbf{k}}} \frac{\tau}{1+\omega^2\tau^2} \right\}, \quad (4) \end{aligned}$$

where we have dropped a small term associated with the derivative of the d-wave form factor $\varphi_{\mathbf{k}}^2$. Here $\Delta_{\text{sc},\pm} = \Delta_{\text{sc}}(T)\varphi_{\mathbf{k}\pm\mathbf{q}/2}$ and $\Delta_{\text{pg},\pm} = \Delta_{\text{pg}}(T)\varphi_{\mathbf{k}\pm\mathbf{q}/2}$. Because of their complexity, we do not include self-consistent impurity effects, which, due to bosonic contributions, will require a modification of earlier work²¹ predicting d-wave fermionic quasiparticles in the ground state. Moreover, it seems plausible that noncondensed pairs may also be associated with these impurity effects, thereby leading to incomplete condensation and finite Δ_{pg} in the ground state. In general, our calculations tend to underestimate the very low T spectral weight away from $\omega = 0$.

III. NUMERICAL RESULTS

The upper panel in Fig. 1 displays a decomposition of the normal state conductivity versus ω . The top curve is $\text{Re}\sigma(\omega)$, while the shaded (red) region labeled ‘‘PG’’ indicates the contribution from noncondensed pairs arising from the F_{pg} terms in Eq. (1). This figure shows clearly what is implicit in Eq. (4), namely, that these pseudogap effects transfer spectral weight from low to high ω . Here the inset plots the resistivity as a function of T .

The lower panel in Fig. 1 plots the real part of the optical conductivity versus ω at the four different temperatures $T/T_c = 1.2, 0.8, 0.4,$ and 0.2 . There are two peak structures in these plots, the lower Drude-like peak, from the quasiparticle-scattering contribution and the upper peak associated with the breaking of preformed pairs. The ‘‘PG’’ contribution disappears at the lowest temperatures, as all pairs go into the condensate. Thus one sees in the figure once the condensate is formed below T_c , the low-frequency peak narrows and increases in magnitude. Conversely, the proportion of the spectral weight residing at high energies on the order of 10^3 cm^{-1} increases with temperature.

To more deeply analyze this redistribution of spectral weight, the difference of the frequency integrated conductivity between $1.4T_c$ and $0.6T_c$ of the present theory is plotted as a function of ω/t in the inset of the bottom panel in Fig. 1. Here we define $W(\omega, T) = (2/\pi) \int_0^\omega d\omega' \sigma(\omega', T)$ and $\Delta W(\omega) = W(\omega, 1.4T_c) - W(\omega, 0.6T_c)$. For comparison, we plot a counterpart ‘‘BCS-like’’ spectral weight change which is derived by effectively neglecting the terms involving Δ_{pg}^2 in Eq. (4). Both conductivities are normalized by their independently calculated change in superfluid densities, $\Delta n_s/m$. The present theory leads to the full integrated (normalized) spectral weight by $\omega \approx 1 \text{ eV}$, while the BCS-like curve counterpart corresponds to $\omega \approx 60 \text{ meV}$. One can see that the presence of noncondensed pairs redistributes an appreciable amount of spectral weight to higher energies. Experimentally, there

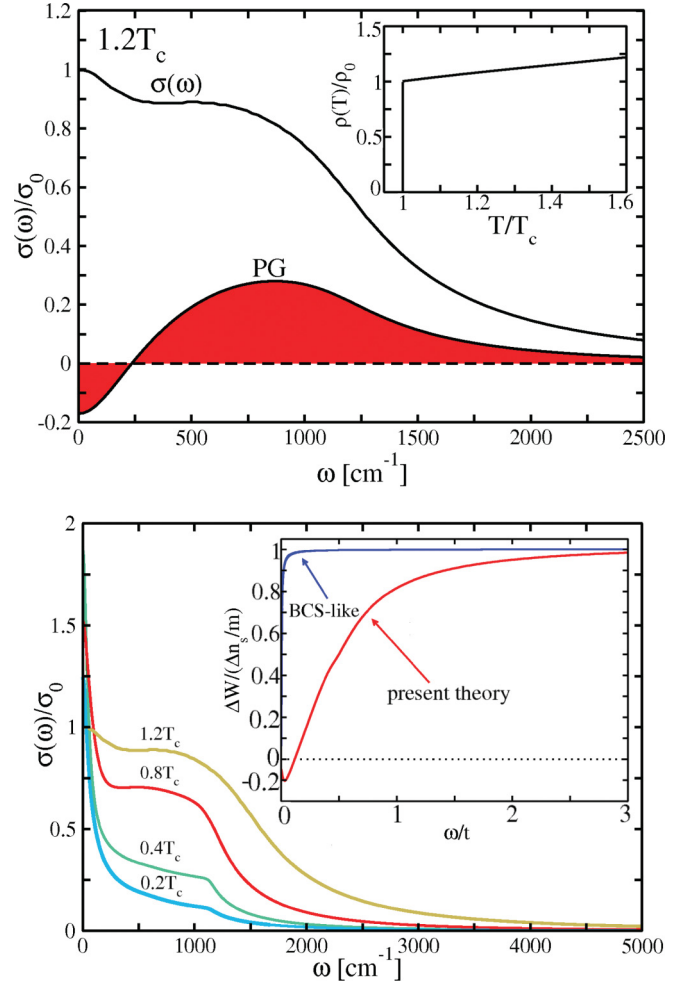


FIG. 1. (Color online) Upper panel (top) curve plots $\text{Re}\sigma(\omega)$ for $T = 1.1T_c$, while the shaded (red) area labeled ‘‘PG’’ shows the transfer of spectral weight from low to higher ω associated with noncondensed pairs. Inset shows the dc resistivity. Lower panel plots $\sigma(\omega)$ at different indicated temperatures. Normalization is $\sigma_0 = \sigma(0)$ at $1.2T_c$. The inset shows the difference of spectral weight between 1.4 and $0.6T_c$ normalized by the difference in superfluid densities. The present theory (red) is contrasted with a BCS-like case (blue) where all explicit Δ_{pg} contributions are dropped.

have been claims that very high energy scales ranging from 1.5 to 2 eV may be needed to satisfy the sum rule. This figure shows how pseudogap contributions can be, at least partly, responsible for these high-energy scales.

We present a more detailed set of comparisons between theory and experiment in Fig. 2, where, for the latter, we reproduce the $y = 6.75$ plots in Fig. 4 from Ref. 2 in panels (a)–(c) and the bottom panel of Fig. 5 from the same work in panel (d). Panels (e)–(g) in Fig. 2 are associated with $T/T_c = 1.4, 0.4,$ and 0.2 and should be compared with the plots in (a)–(c). Here one sees rather similar trends. Importantly the Drude peak narrows and increases in height as T decreases. The MIR peak position is relatively constant, (as seen experimentally) and in the theory roughly associated with 2Δ , the value of which is identified in each panel (e)–(g). That $\Delta(T)$ is roughly constant through the displayed temperature range, reflects the interconversion of noncondensed to condensed pairs.

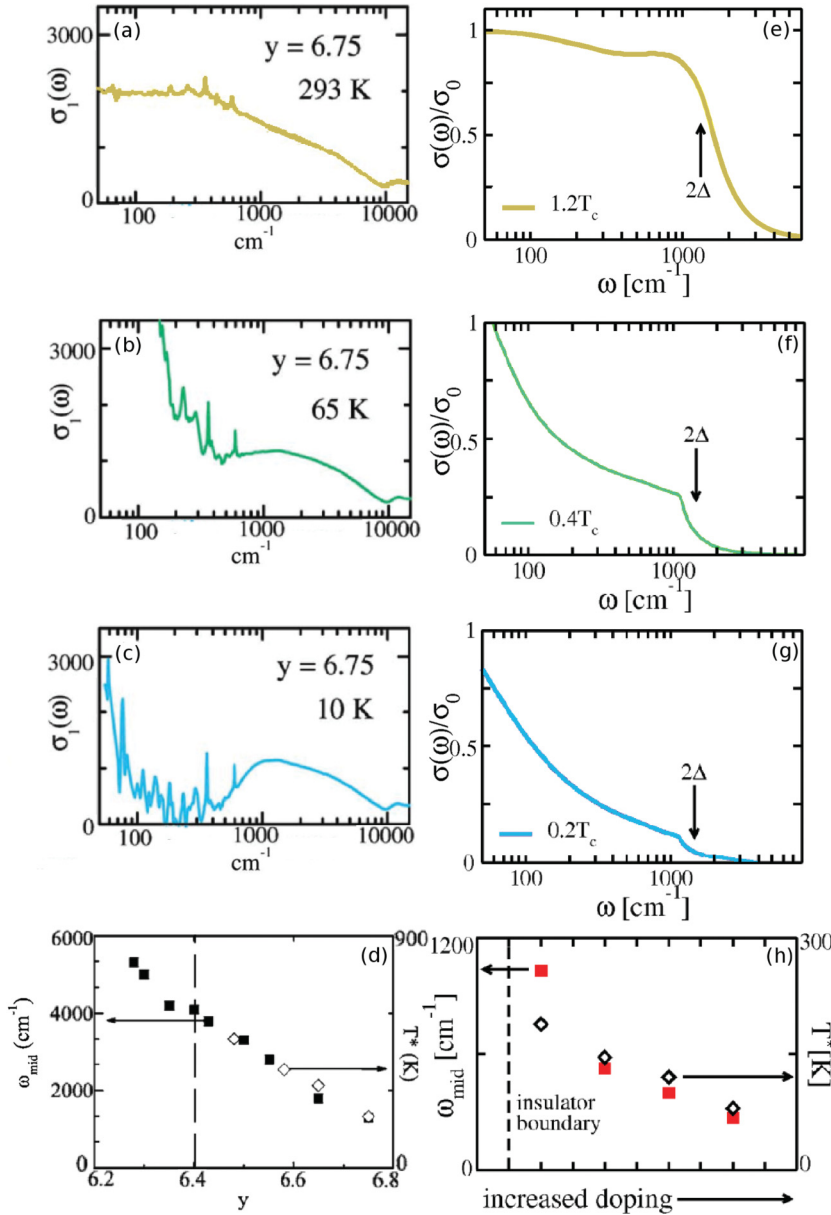


FIG. 2. (Color online) The left column consists of figures reproduced from Ref. 2 and is to be contrasted with the corresponding theoretical results in the right column. Panels (a)–(c) show the optical conductivity for decreasing temperature, and panel (d) plots the MIR peak location ω_{mid} and T^* as a function of doping. The theoretical results in (e)–(g) show the optical conductivity for $T/T_c = 1.2, 0.4$, and 0.2 where $\sigma(\omega)$ is normalized by $\sigma_0 = \sigma(0)$ at $T = 1.2T_c$. The final panel (h) displays ω_{mid} and T^* as functions of doping. A dashed line in plots (d) and (h) indicates the insulator boundary, which represents the limit of validity for our theory.

It should be noted, however, that the height of the MIR peak in the data is more temperature independent than found in theory. This would seem to suggest that there are noncondensed pair states at $T = 0$ perhaps associated with inhomogeneity or localization²¹ effects. This interpretation of the optical data appears consistent with our previous studies²² of angle-resolved photoemission (ARPES) data from which we have inferred that the ground state in strongly underdoped samples may not be the fully condensed d-wave BCS phase. Rather there may be some noncondensed pair or pseudogap effects which persist to $T = 0$. In ARPES experiments one could attribute this persistence to the fact that the $T = 0$ gap shape is distorted relative to the more ideal d-wave form found in moderately underdoped systems.²³ Similar observations are made from STM experiments.²⁴

We show in Fig. 2(h) a plot of the MIR peak location ω_{mid} as a function of T^* as calculated in our theory; this plot suggests that the MIR peak position scales (nearly linearly)

with the pairing gap or equivalently with T^* . This observation is qualitatively similar (within factors of 2 or 3) to Fig. 2(d), reproduced from Ref. 2. Finally, we stress that we have investigated the effects of varying γ as well as its T dependence and find that our results in Fig. 2 remain very robust, as shown in the Appendix.

IV. CONCLUSIONS

At the core of interest in the optical conductivity is what one can learn about the origin of the pseudogap. We earlier discussed problematic aspects of alternative scenarios for the two-component optical response. We reiterate that the observed tight correlation with the two-component optical response and the presence of a pseudogap² is natural in the present theory, where the MIR peak is to be associated directly with the breaking of metastable pairs. Such a contribution does not disappear below T_c , until all pairs

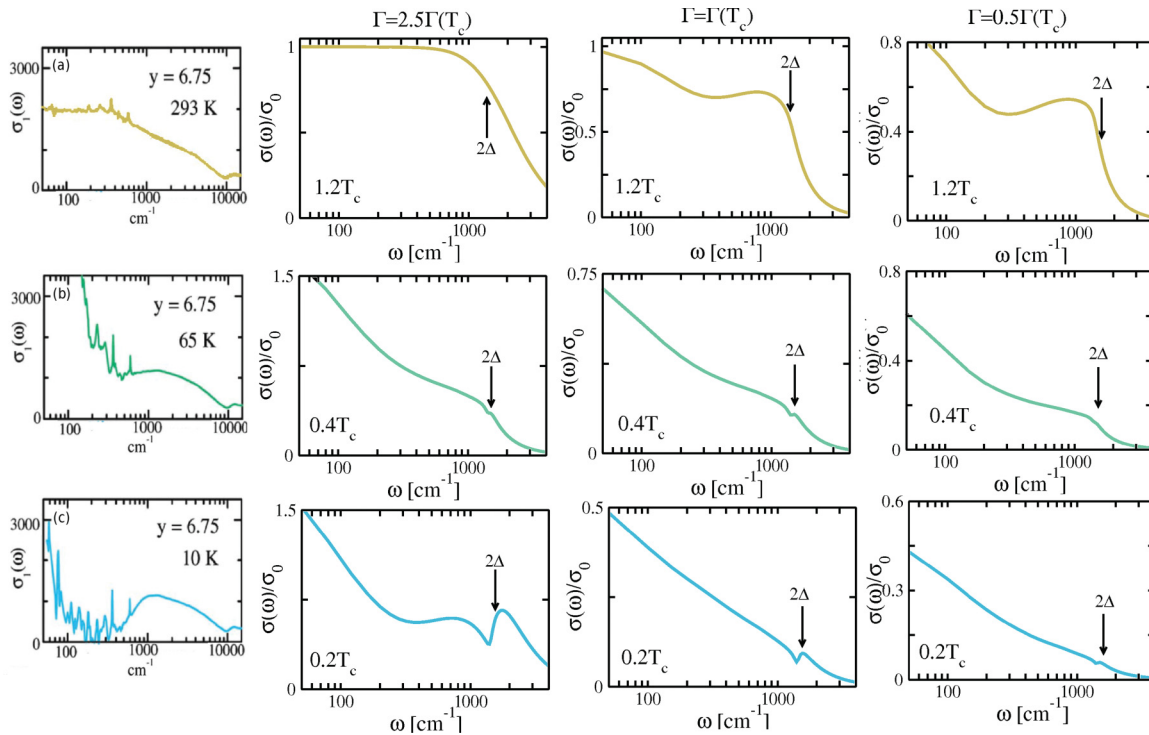


FIG. 3. (Color online) Illustrative figure for the case of constant gamma. The numerical values indicated are quoted relative to those we showed in the paper.

are condensed. In summary, our paper appears compatible with the very important experimental conclusion in Ref. 2 that “Our findings suggest that any explanation [of the MIR peak] should take into account the correlation between the formation of the mid IR absorption and the development of the pseudogap.”

ACKNOWLEDGMENTS

This work is supported by NSF-MRSEC Grant 0820054. C.C.C. acknowledges the support of the US Department of Energy through the LANL/LDRD Program.

APPENDIX: FURTHER NUMERICAL STUDIES

In this appendix we present a comparison figure, Fig. 3, for the optical conductivity in the case where we take the parameter γ to be constant in temperature for three different values of γ . The first column in Fig. 3 reproduces the experimental data from Ref. 2. The remaining columns show the theoretical data for decreasing values of γ . Each row corresponds to decreasing temperature from top to bottom. This shows that the results are robust over a large range of γ and very much independent of what values or temperature dependencies are assumed for the lifetime broadening.

¹D. N. Basov and T. Timusk, *Rev. Mod. Phys.* **77**, 721 (2005).

²Y. S. Lee, K. Segawa, Z. Q. Li, W. J. Padilla, M. Dumm, S. V. Dordevic, C. C. Homes, Y. Ando, and D. N. Basov, *Phys. Rev. B* **72**, 054529 (2005).

³A. F. Santander-Syro, R. P. S. M. Lobo, N. Bontemps, W. Lopera, D. Girata, Z. Konstantinovic, Z. Z. Li, and H. Raffy, *Phys. Rev. B* **70**, 134504 (2004).

⁴K. Kamaras, S. L. Herr, D. Porter, N. Tache, D. B. Tanner, S. Etemad, T. Venkatesan, E. Case, A. Inam, X. D. Wu *et al.*, *Phys. Rev. Lett.* **64**, 84 (1990).

⁵Q. J. Chen, J. Stajic, S. Tan, and K. Levin, *Phys. Rep.* **412**, 1 (2005).

⁶I. Kosztin, Q. J. Chen, Y.-J. Kao, and K. Levin, *Phys. Rev. B* **61**, 11662 (2000).

⁷Q. J. Chen, I. Kosztin, B. Jankó, and K. Levin, *Phys. Rev. Lett.* **81**, 4708 (1998).

⁸H. Guo, C.-C. Chien, and K. Levin, *Phys. Rev. Lett.* **105**, 120401 (2010).

⁹D. Wulin, B. M Fregoso, H. Guo, C.-C. Chien, and K. Levin, *Phys. Rev. B* **84**, 140509(R) (2011).

¹⁰N. Lin, E. Gull, and A. J. Millis, *Phys. Rev. B* **80**, 161105(R) (2009).

¹¹L. Benfatto, S. G. Sharapov, N. Andrenacci, and H. Beck, *Phys. Rev. B* **71**, 104511 (2005).

¹²L. Benfatto and S. G. Sharapov, *Low Temp. Phys.* **32**, 533 (2006).

¹³J. Orenstein, in *Handbook of High-Temperature Superconductivity: Theory and Experiment*, edited by J. R. Schrieffer and J. S. Brooks (Springer, New York, 2007), p. 299.

¹⁴L. S. Bilbro, R. V. Aguilar, G. Logvenov, O. Pelleg, I. Božović, and N. P. Armitage, *Nature Phys.* **7**, 298 (2011).

¹⁵G. Deutscher, A. F. Santander-Syro, and N. Bontemps, *Phys. Rev. B* **72**, 092504 (2005).

- ¹⁶J. Maly, B. Jankó, and K. Levin, *Physica C* **321**, 113 (1999).
- ¹⁷J. Maly, B. Jankó, and K. Levin, *Phys. Rev. B* **59**, 1354 (1999).
- ¹⁸M. R. Norman, M. Randeria, H. Ding, and J. C. Campuzano, *Phys. Rev. B* **57**, R11093 (1998).
- ¹⁹A. V. Chubukov, M. R. Norman, A. J. Millis, and E. Abrahams, *Phys. Rev. B* **76**, 180501(R) (2007).
- ²⁰T. Senthil and P. A. Lee, *Phys. Rev. B* **79**, 245116 (2009).
- ²¹P. A. Lee, *Phys. Rev. Lett.* **71**, 1887 (1993).
- ²²C.-C. Chien, Y. He, Q. Chen, and K. Levin, *Phys. Rev. B* **79**, 214527 (2009).
- ²³W. S. Lee, I. M. Vishik, K. Tanaka, D. H. Lu, T. Sasagawa, N. Nagaosa, T. P. Devereaux, Z. Hussain, and Z. X. Shen, *Nature (London)* **450**, 81 (2007).
- ²⁴A. Pushp, C. Parker, N. Pasupathy, K. K. Gomes, S. Ono, J. Wen, Z. Xu, G. Gu, and A. Yazdani, *Science* **324**, 1689 (2009).